University of Dayton
eCommons

Chemistry Faculty Publications

Department of Chemistry

1986

A Theoretical Investigation of the One– and Two–photon Properties of Porphyrins

Mark Masthay
University of Dayton, mmasthay1@udayton.edu

Leonore A. Findsen
Syracuse University

Brian M. Pierce
Carnegie Mellon University

David F. Bocian
Carnegie Mellon University

James S. Lindsey
Carnegie Mellon University

See next page for additional authors

Follow this and additional works at: https://ecommons.udayton.edu/chm_fac_pub

Part of the Other Chemistry Commons, and the Physical Chemistry Commons

Author(s)
Mark Masthay, Leonore A. Findsen, Brian M. Pierce, David F. Bocian, James S. Lindsey, and Robert R. Birge

A theoretical investigation of the one- and two-photon properties of porphyrins

M. B. Masthay, L. A. Findsen, B. M. Pierce, D. F. Bocian, J. S. Lindsey, and R. R. Birge
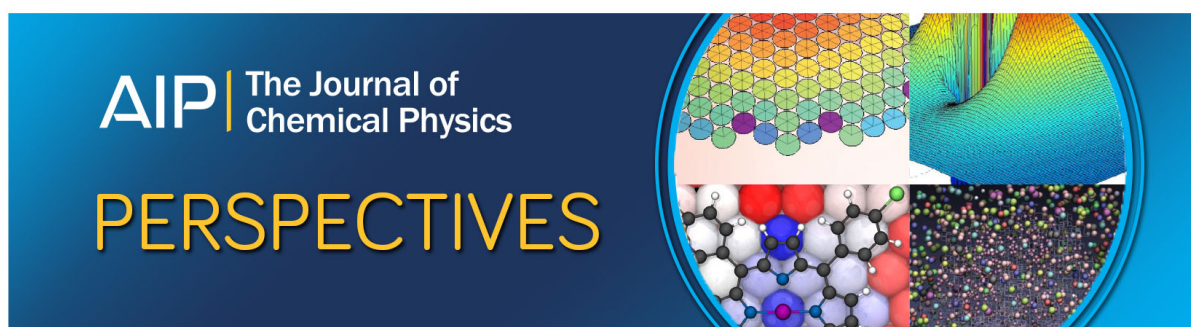
A theoretical investigation of the one- and two-photon properties of porphyrins[a]

M. B. Masthay, L. A. Findsen, B. M. Pierce, D. F. Bocian, J. S. Lindsey, and R. R. Birge[b]

Department of Chemistry, Carnegie–Mellon University, Pittsburgh, Pennsylvania 15213

The one- and two-photon properties of free base porphin, free base porphin dianion, and the 2,4-substituted diformyl and divinyl analogs of these molecules are studied using a semiempirical SCF-MO formalism (CNDO-π-SCF-MO-PSDCI) including extensive single and double configuration interaction. Strongly two-photon allowed states are predicted to lie in the Soret region as well as in the region between the Soret and visible bands. A number of the two-photon allowed states in the Soret region are predicted to have two-photon absorptivities exceeding 100×10^{-50} cm^4 s molecule^{-1} photon^{-1}. The calculations indicate that the visible (Q) states are well characterized by the four orbital model, whereas the Soret (B) states contain significant contributions from configurations comprised of other orbitals. The inclusion of extensive double configuration interaction significantly reduces the Soret-visible (B–Q) splitting, increases the Q_x–Q_y splitting, and yields calculated oscillator strengths for the Q bands in better agreement with experiment than values calculated using single CI alone. The effects of conjugation into the porphyrin macrocycle are predicted to be more significant than inductive effects on macrocycle π orbitals due to substituent polarity. The $\langle Q_x |\mathbf{r}| S_0 \rangle$ and $\langle Q_y |\mathbf{r}| S_0 \rangle$ transition moment vectors are predicted to lie approximately through adjacent pyrrole rings in 2- and 4-monoformyl free base porphin dianions and approximately through adjacent methine bridges in 2,4-diformyl free base porphin dianion.

I. INTRODUCTION

Porphyrins and their analogs participate in a wide variety of important biological processes, including oxygen and electron transport (the hemes) and photosynthesis (the chlorophylls). Consequently, much theoretical effort has been exerted in attempts to elucidate the electronic properties of these molecules.[1-18] The fundamental units from which all porphyrins derive their structure are free base porphin (FBP) and free base porphin dianion (FBP^{2-}). Many biologically significant porphyrins are derivatives of these two molecules with vinyl or formyl substituents in various positions on the porphyrin macrocycle (see Fig. 1).

Previous theoretical investigations of porphyrins have concentrated on the calculation of the one-photon properties, although the potential significance of two-photon allowed states has been noted.[5,8,15] Two-photon spectroscopy has proved to be of great utility in studying the electronic properties of the linear polyenes and benzenoid hydrocarbons. The results presented here suggest that two-photon spectroscopy will be very useful for evaluating the electronic excited states of the porphyrins as well.

Although the principal goal of this study is to evaluate the two-photon properties of the $\pi\pi^*$ excited states of porphyrins, secondary goals include an analysis of the importance of electron correlation and the effect of conjugating substituents on the spectroscopic properties of porphyrins. The mechanisms by which conjugating substituents influence the spectroscopic properties of porphyrins are not well understood. Calculations were carried out on unsubstituted and substituted species in order to gain insight into these mechanisms. The electronic excited states of FBP and FBP^{2-} are evaluated first, with a discussion of the effects of including extensive double configuration interaction, followed by an evaluation of the 2,4-divinyl and 2,4-diformyl substituted species. The possible roles which conjugation into the π system of the macrocycle and inductive effects on porphyrin π orbitals by polar substituents may play in influencing one-photon oscillator strengths, state energies, and the Q_x and Q_y transition moment polarizations are evaluated. The possible roles of solvent-induced perturbations on the spectra of substituted species (with respect to their unsubstituted parent molecules) are also evaluated. The effects of static external electric fields on the spectra of porphyrins are also theoretically determined and compared with those induced by polar substituents.

A procedure for calculating the two-photon properties of large molecules which is both rigorous and computationally tractable is not available. The orientationally averaged CNDO-π-SCF-MO-PSDCI molecular orbital formalism utilized in this paper is, however, an improvement over the technique employed in earlier theoretical two-photon investigations,[19] and we have attempted to quantify the sources of error in our method. Our procedures are predicted to offer order of magnitude estimates of two-photon absorptivities. The present lack of experimentally observed absolute two-photon absorptivities for porphyrins prevents a comprehensive analysis at this time. The calculated relative values of the two-photon absorptivities and the predicted polarizations are expected to be much more accurate than the absolute values, however, and should prove useful to researchers us-
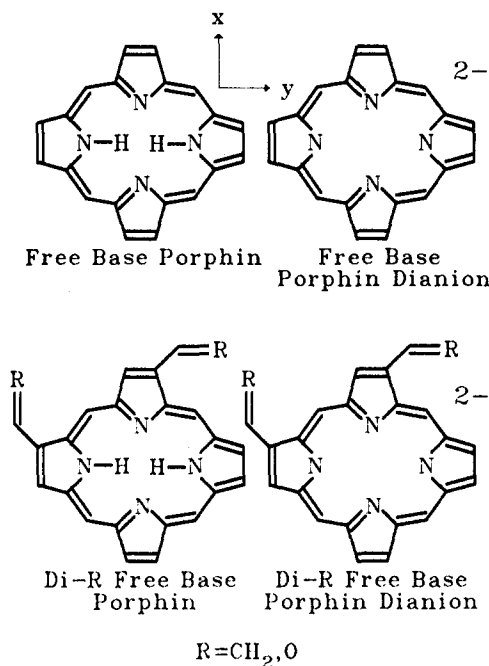
FIG. 1. Free base porphin, free base porphin dianion, and their 2,4-diformyl and 2,4-divinyl analogs.

ing two-photon spectroscopy to analyze the photophysical properties of porphyrins.

II. THEORETICAL

A. Molecular orbital calculations

The excited state transition energies and transition lengths appearing in Eqs. (2) and (6)–(9) were evaluated using a self-consistent field molecular orbital formalism utilizing π orbitals within the CNDO formalism including full single and partial double (extensive, with 350–400 doubly excited configurations) configuration interaction.[20] The molecular orbital procedures are identical to those used in a previous theoretical investigation on the two-photon properties of linear polyenes,[19] with the exception that overlap is explicitly introduced and the Mataga–Nishimoto formula is used in place of the Ohno formula for calculating the two-center repulsion integrals. Inclusion of extension double CI is particularly important when calculating two-photon properties because the relative ordering of one- and two-photon allowed states in conjugated systems is strongly dependent on the amount of double CI included in the calculations.[21–24] The transition energies (E_i, E_j) are calculated relative to the correlated (SCF) ground state, as correlated transition energies are found to correspond more closely to experimental values than do uncorrelated energies. In calculating two-photon properties, the energies of the two photons are assumed to be equal and are determined by dividing the final state transition energy by two (i.e., $E_\lambda = E_\mu = E_f/2$). In performing field effect calculations, the field induced perturbation is introduced into the diagonal elements of the Fock Hamiltonian

$$F_{\mu\mu} = -I_\mu + \tfrac{1}{2}P_{\mu\mu}\langle\mu\mu|\mu\mu\rangle$$

$$+ \sum_{\nu\neq\mu}(P_{\nu\nu} - z_\nu)\langle\mu\mu|\nu\nu\rangle - eE_x x_\mu, \quad (1)$$

where E_x is the electric field strength, the x_μ is the Cartesian coordinate of the μth atom, along the x axis.[25] The remaining terms are defined in Ref. 26. Although the above procedure is appropriate for static external fields of moderate intensity, an accurate treatment of high fields would require the inclusion of second order terms, and a proper description of laser induced effects would require explicit consideration of the radiation field Hamiltonian. Nevertheless, Eq. (1) is sufficiently accurate for the semiquantitative discussion that follows.

Coordinates used for the porphyrin ring in all molecules studied are taken from x-ray data for tetraphenylporphyrins[27] artificially constrained to planarity.[6–8] Standard geometries are used for vinyl and formyl groups, and these substituents are assumed to be coplanar with the porphyrin ring.

B. One-photon properties

The one-photon oscillator strengths for transitions from the ground state (0) to the final state (f) are calculated utilizing the standard expression for theoretical oscillator strength[26]:

$$f_{f0} = \frac{8\pi^2 mc}{3h}\tilde{\nu}_{f0}\,|\langle f|r|0\rangle|^2, \quad (2)$$

where m is the electron rest mass, c is the speed of light, h is Planck's constant, $\tilde{\nu}_{f0}$ is the transition energy in wave numbers, and $\langle f|r|0\rangle$ is the transition dipole length.

C. Two-photon properties

The two-photon absorptivity for a transition from the ground electronic state (0) into a final excited state (f) is proportional to the molecular two-photon tensor[19,28–33]

$$|S_{f0}(\lambda,\mu)|^2 = \left|\sum_i^N\left[\frac{(\lambda\cdot\langle i|r|0\rangle)(\langle f|r|i\rangle\cdot\mu)}{E_i - E_\lambda + i\Gamma_i}\right.\right.$$

$$\left.\left.+ \frac{(\mu\cdot\langle i|r|0\rangle)(\langle f|r|i\rangle\cdot\lambda)}{E_i - E_\mu + i\Gamma_i}\right]\right|^2, \quad (3a)$$

where λ and μ are the unit vectors defining the polarization of the two photons, $\langle j|r|i\rangle$ is a transition $(i\neq j)$ or dipole $(i = j)$ length vector, E_λ and E_μ are the energies of photon λ and photon μ, respectively, and E_i and Γ_i are the energy and the linewidth, respectively, associated with the ith state. N is the total number of intermediate states and the summation includes the ground and final states (see below). Equation (3a) can be rewritten in the following form to facilitate evaluation[31]:

$$|S_{f0}(\lambda,\mu)|^2 = P(\lambda,\mu)\theta(\alpha,\beta,\rho,\sigma)(S_{\alpha\beta}S^*_{\rho\sigma}), \quad (3b)$$

where $P(\lambda,\mu)$ defines the polarization of the λ and μ photons, $\theta(\alpha,\beta,\rho,\sigma)$ defines the molecular orientation of the absorbing species relative to the photon polarization and propagation vectors, and $(S_{\alpha\beta}S^*_{\rho\sigma})$ is a product of two second-rank tensors which are functions of the internal molecular Cartesian coordinates α and β and the photon and state energies

$$S_{\alpha\beta} = \sum_i^N \left[\frac{\langle i|\alpha|0\rangle \langle f|\beta|i\rangle}{E_i - E_\lambda + i\Gamma_i} + \frac{\langle i|\beta|0\rangle \langle f|\alpha|i\rangle}{E_i - E_\mu + i\Gamma_i} \right], \qquad (4)$$

where $\langle j|\alpha|i\rangle$ represents a transition $(i \neq j)$ or dipole $(i = j)$ length along the α (molecular coordinate) axis.

Monson and McClain have developed a closed form expansion applicable to randomly oriented absorbing species which reduces Eq. (3b) to the following form[31]:

$$|S_{f0}(\lambda,\mu)|^2 = (1/30) [f(S_{\alpha\alpha}S^*_{\beta\beta})$$
$$+ g(S_{\alpha\beta}S^*_{\alpha\beta}) + h(S_{\alpha\beta}S^*_{\beta\alpha})], \qquad (5)$$

where f, g, and h are real variables which define the relative photon polarization and propagation relationships. The subscripts α and β represent the molecular Cartesian axes and indicate summation over all x, y, and z. It should be noted that Eq. (5) retains generality in that any two-photon excitation arrangement can be specified by an appropriate choice of f, g, and h. Some examples taken from a larger list compiled by Monson and McClain are given in Table I. The symbols $\langle A\rangle$ through $\langle D\rangle$ will be used throughout this paper to refer to specific photon relationships.

The tensor products on the right-hand side of Eq. (5) are defined as double sums over all the steady state electronic levels of the molecule including the ground and final states

$$S_{\alpha\alpha}S^*_{\beta\beta} = \sum_i^N \sum_j^N \Big((\langle i|\mathbf{r}|0\rangle \cdot \langle f|\mathbf{r}|i\rangle)(\langle j|\mathbf{r}|0\rangle \cdot \langle f|\mathbf{r}|j\rangle)$$
$$\times \{ [((E_i - E_\lambda)((E_j - E_\lambda) + \Gamma^2]^{-1}$$
$$+ 2[(E_i - E_\lambda)(E_j - E_\mu) + \Gamma^2]^{-1}$$
$$+ [(E_i - E_\mu)(E_j - E_\mu) + \Gamma^2]^{-1} \} \Big), \qquad (6)$$

$$S_{\alpha\beta}S^*_{\alpha\beta} = \sum_i^N \sum_j^N \left\{ \frac{(\langle i|\mathbf{r}|0\rangle \cdot \langle j|\mathbf{r}|0\rangle)(\langle f|\mathbf{r}|i\rangle \cdot \langle f|\mathbf{r}|j\rangle)}{[(E_i - E_\lambda)(E_j - E_\lambda) + \Gamma^2]} + \frac{(\langle i|\mathbf{r}|0\rangle \cdot \langle j|\mathbf{r}|0\rangle)(\langle f|\mathbf{r}|i\rangle \cdot \langle f|\mathbf{r}|j\rangle)}{[(E_i - E_\mu)(E_j - E_\mu) + \Gamma^2]} \right.$$
$$\left. + \frac{(\langle i|\mathbf{r}|0\rangle \cdot \langle f|\mathbf{r}|j\rangle)(\langle f|\mathbf{r}|i\rangle \cdot \langle j|\mathbf{r}|0\rangle)}{[(E_i - E_\lambda)(E_j - E_\mu) + \Gamma^2]} + \frac{(\langle i|\mathbf{r}|0\rangle \cdot \langle f|\mathbf{r}|j\rangle)(\langle f|\mathbf{r}|i\rangle \cdot \langle j|\mathbf{r}|0\rangle)}{[(E_i - E_\mu)(E_j - E_\lambda) + \Gamma^2]} \right\}, \qquad (7)$$

$$S_{\alpha\beta}S^*_{\beta\alpha} = \sum_i^N \sum_j^N \left\{ \frac{(\langle i|\mathbf{r}|0\rangle \cdot \langle j|\mathbf{r}|0\rangle)(\langle f|\mathbf{r}|i\rangle \cdot \langle f|\mathbf{r}|j\rangle)}{[(E_i - E_\lambda)(E_j - E_\mu) + \Gamma^2]} + \frac{(\langle i|\mathbf{r}|0\rangle \cdot \langle j|\mathbf{r}|0\rangle)(\langle f|\mathbf{r}|i\rangle \cdot \langle f|\mathbf{r}|j\rangle)}{[(E_i - E_\mu)(E_j - E_\lambda) + \Gamma^2]} \right.$$
$$\left. + \frac{(\langle i|\mathbf{r}|0\rangle \cdot \langle f|\mathbf{r}|j\rangle)(\langle f|\mathbf{r}|i\rangle \cdot \langle j|\mathbf{r}|0\rangle)}{[(E_i - E_\lambda)(E_j - E_\lambda) + \Gamma^2]} + \frac{(\langle i|\mathbf{r}|0\rangle \cdot \langle f|\mathbf{r}|j\rangle)(\langle f|\mathbf{r}|i\rangle \cdot \langle j|\mathbf{r}|0\rangle)}{[(E_i - E_\mu)(E_j - E_\mu) + \Gamma^2]} \right\}. \qquad (8)$$

In contrast to earlier studies,[19,28] our calculations include initial and final states in the summations of Eqs. (6)–(8). More recent studies[34–36] have demonstrated the importance of including initial and final state contributions to the two-photon tensor elements for molecules in which there is a change in dipole moment upon excitation, as is the case for many of the molecules studied in this paper. In Eqs. (6)–(8), Γ is now interpreted as a damping constant appropriate for a typical excited state linewidth or energy uncertainty, whichever is larger (see below).

TABLE I. Photon polarization and propagation relationships.

Symbol	f[Eq. (5)]	g[Eq. (5)]	h[Eq. (5)]	a[Eq. (9)]	b[Eq. (9)]
$\langle A\rangle$[a]	2	2	2	8	8
$\langle B\rangle$[b]	−1	4	−1	−4	6
$\langle C\rangle$[c]	−2	3	3	−8	12
$\langle D\rangle$[d]	3	3	−2	12	2

[a] Both photons linearly polarized with parallel polarization.
[b] Both photons linearly polarized with perpendicular polarization or one photon circularly polarized, the other linearly polarized perpendicular to the plane of circular polarization.
[c] Both photons circularly polarized in the same sense with parallel propagation.
[d] Both photons circularly polarized in the opposite sense with parallel propagation.

As previously noted by Birge and Pierce, Eq. (5) is significantly simplified when both photons have the same energy $(E_\lambda = E_\mu)$[19,28]:

$$|S_{f0}(\lambda,\lambda)|^2 = \frac{1}{30} \sum_i^N \sum_j^N S_{ij}^{(f)}, \qquad (9a)$$

where

$$S_{ij}^{(f)} = \left\{ \frac{a(\langle i|\mathbf{r}|0\rangle \cdot \langle f|\mathbf{r}|i\rangle)(\langle j|\mathbf{r}|0\rangle \cdot \langle f|\mathbf{r}|j\rangle)}{[(E_i - E_\lambda)(E_j - E_\lambda) + \Gamma^2]} \right.$$
$$+ \frac{b(\langle i|\mathbf{r}|0\rangle \cdot \langle j|\mathbf{r}|0\rangle)(\langle f|\mathbf{r}|i\rangle \cdot \langle f|\mathbf{r}|j\rangle)}{[(E_i - E_\lambda)(E_j - E_\lambda) + \Gamma^2]}$$
$$\left. + \frac{b(\langle i|\mathbf{r}|0\rangle \cdot \langle f|\mathbf{r}|j\rangle)(\langle f|\mathbf{r}|i\rangle \cdot \langle j|\mathbf{r}|0\rangle)}{[(E_i - E_\lambda)(E_j - E_\lambda) + \Gamma^2]} \right\}. \qquad (9b)$$

Only two variables, a and b, are now necessary to specify the possible photon relationships (see Table I).[19,28]

The transition energies calculated using the CNDO-π-SCF-MO-PSDCI procedures are approximate. Consequently, unrealistically large calculated two-photon absorptivities can result from accidental resonances in the denominator of Eq. (9) associated with higher energy excited states. A large damping constant of $\Gamma = 0.05$ eV was used to prevent fortuitous resonances from "blowing up." The absorptivities calculated for the higher energy states are potentially much less accurate than those calculated for the low-lying transitions.

The two-photon absorptivity δ_{f0} (in unit of cm^4 s molecule^{-1} photon^{-1} is calculated using Eq. (10)[29–31]:

$$\delta_{f0} = \frac{(2\pi e)^4}{(ch)^2}[E_\lambda E_\mu g(E_\lambda + E_\mu)] \, |S_{f0}|^2, \qquad (10)$$

where E_λ and E_μ are the energies of the λ and μ photons, respectively, and $g(E_\lambda + E_\mu)$ is the normalized line shape function, proportional to the cross-sectional contour of the final state. Each transition will have a unique line shape function which will be very complicated in those instances where vibronic structure can be resolved. With the exception of the visible bands, the electronic states of the porphyrins in the present paper are not expected to exhibit highly resolved vibrational structure in their absorption spectra. In order to facilitate comparison of calculated absorptivities, including those of the visible bands,[37] we will represent the line shape function for *all* molecules as a Gaussian profile centered at the calculated energy maximum for the final state E_f[19,28]:

$$g(E_\lambda + E_\mu) = g_{\max} \exp\left[\frac{-4\ln 2}{E^2_{\text{FWHM}}}(E_\lambda + E_\mu - E_f)^2\right], \qquad (11)$$

where

$$g_{\max} = (4h^2 \ln 2/\pi E^2_{\text{FWHM}})^{1/2}. \qquad (12)$$

The calculations presented in Sec. III use a $g_{\max}$ of 1.5×10^{-14} s, corresponding to a full width at a half-maximum of approximately 2100 cm^{-1} and assume that two photons of equal energy are absorbed.

D. Sources of error

The calculations presented in the following sections utilize Eqs. (1) and (2) and (9)–(12) and include the 30 lowest singlets as intermediate states in the two-photon tensor elements [i.e., $N = 30$ in Eq. (9a) in all cases]. Initial and final states are included in the summation over intermediate states. The accuracy of our calculations of transition lengths and transition energies is limited by our use of semiempirical basis set CNDO-π-SCF-MO-PSDCI wave functions and our use of idealized geometries. Calculations on dianions (intended to model metalloporphyrins) contain an additional source of error in that they lack metal parametrization. Calculated two-photon absorptivity values contain a further accuracy limitation because of our use of a limited basis set of intermediate states. We discuss these sources of error in more detail in the paragraphs which follow.

Three primary sources of error exist within our formalism. Although semiempirical wave functions tend to overestimate transition lengths, transition lengths are sometimes underestimated with the inclusion of extensive double CI. Furthermore, Soret and visible states are affected differently. In free base porphin for example, the oscillator strength of the Soret bands and the Q_y band are almost identical to the experimental values, whereas the Q_x band exhibits an oscillator strength larger than the experimental value by a factor of 6. Small errors in transition lengths can result in large errors in calculated two-photon properties because of the fourfold product in the numerator of Eq. (9).

The use of idealized porphyrin ring geometries and "standard geometries" for substituent vinyl or formyl groups is a second source of error. The assumption of com-plete planarity tends to cause overestimation or underestimation of transition length vectors for strongly allowed (Soret) or weakly allowed (visible) states, respectively. Furthermore, vinyl or formyl groups in the substituted molecules are assumed to be coplanar with the porphyrin ring. Recent experimental evidence suggests that conjugating substituent groups lie significantly out-of-plane in substituted porphyrins (see Sec. III C). The assumption of coplanarity allows the substituents to conjugate into the porphyrin ring quite strongly, typically causing an underestimation of transition length vectors for allowed states and an overestimation for forbidden states (i.e., selection rule breakdown is overestimated).

A third source of error relates to the use of a limited basis set of intermediate states in the two-photon tensor elements. This source of error has been discussed in detail in Appendix I of Ref. 19. It is sufficient to note that test calculations indicate that 30 intermediate states generate calculated two-photon absorptivities within 20% of the "full" calculation. This error is negligible relative to the other sources discussed.

A fourth source of error relates only to the calculations on porphyrin dianions. In the studies on dianions (which are taken to be representative of metalloporphyrins) we included no metal parameters. Metal parametrization is expected to significantly influence calculated transition energies and transition length vectors. We therefore expect our calculations to be more accurate for the free bases than for the dianions.

Our error analysis suggests therefore that calculated values of two-photon absorptivities should best be viewed as order-of-magnitude estimates. The relative values within a homologous series (the neutral species or the dianions, respectively) are expected to be much more reliable, however, and much of our analysis is based upon comparative rather than absolute values for one-photon oscillator strengths and two-photon absorptivities. The two-photon polarization ratios are expected to be much more accurate as they are primarily dependent upon symmetries of the wave functions and are somewhat insensitive to intermediate basis set size and absolute magnitudes of the calculated transition lengths.

As an illustration of the expected direction and magnitude of error we draw upon the following example taken from research on retinyl polyenes. Birge *et al.* report an experimentally measured two-photon absorptivity of $25 \pm 16 \times 10^{-50}$ cm^4 s molecule^{-1} photon^{-1} at the excitation maximum of the lowest excited "$^1A^{*-}_g$" state of all-*trans* retinol.[28] Birge and Pierce, using a technique similar to that used in this paper, calculated an absorption maximum of 30×10^{-50} cm^4 s molecule^{-1} photon^{-1} for the same transition,[19] well within the range of experimental error. It should be noted, however, that the lowest-lying forbidden states of polyenes are well described using the single intermediate state approximation and are particularly amendable to the calculational approach used here.

III. RESULTS AND DISCUSSION
A. The symmetric porphyrins

Planar free base porphin (FBP) and free base porphin dianion (FBP^{2-}) belong to the D_{2h} and D_{4h} point groups,

respectively. Accordingly, the in-plane one-photon allowed states are of $^1B_{2u}^*$ and $^1B_{3u}^*$ (D_{2h}) and $^1E_u^*$ (D_{4h}) symmetries. In-plane two-photon allowed states belong to the $^1A_g^*$ and $^1B_{1g}^*$ (D_{2h}) and $^1A_g^*$, $^1B_{1g}^*$, and $^1B_{2g}^*$ (D_{4h}) irreducible representations (selection rules are tabulated in Table II).

Calculated one-photon oscillator strengths and two-photon absorptivities for FBP and FBP^{2-} are given in Tables III and IV, respectively. A comparison of transition energies, one-photon oscillator strengths, and two-photon absorptivities for FBP under complete single CI and complete single–extensive double CI is presented in Fig. 2 and Table V. The inclusion of double CI results in a significant reduction of B–Q energy splitting and an increase in Q_x–Q_y energy splitting and Q/B and Q_y/Q_x intensity ratios. The calculated values for the Q–B splitting and the Q_y/Q_x intensity ratio for FBP obtained using single plus double CI are

more accurate than values calculated using single CI alone. Although the addition of double CI does not always improve correlation between theory and experiment for individual transition energies, double CI improves *relative* values of the transition energies for all molecules studied with one exception: the Q_x–Q_y splitting in the free bases. Comparisons of absolute and relative oscillator strengths with experimental values are less reliable because existing data in the literature generally include ϵ_{max} values but do not include bandwidths. No clear trend is apparent for the effect of double CI on relative one-photon oscillator strengths; although there is improvement, in some cases single plus double CI results are less accurate than single CI results.

In accord with earlier semiempirical[5] and *ab initio*[15,17] studies, we find the Q bands to be well described by the four orbital model (88% and 90% four orbital localized in FBP

TABLE II. Optical characteristics of porphyrin excited $\pi\pi^*$ singlet states for the D_{4h}, D_{2h}, and C_s point groups.

Point group	Symmetry (parent)[a]	One photon (polarization)[b]	Two photon (polarization)[c]
D_{4h}	$^1E_u^*$	Weak [visible (Q)]	Forbidden
	$^1E_u^*$	Strongly allowed [Soret (B)]	Forbidden
	$^1B_{1g}^*$	Forbidden	Allowed ($\Omega = 1.5$)
	$^1B_{2g}^*$	Forbidden	Strongly allowed ($\Omega = 1.5$)
	$^1A_{1g}^*$	Forbidden	Strongly allowed ($\Omega = 0.25$)
D_{2h}	$^1B_{2u}^*(^1E_u^*)$	Weak ($\theta \cong 90°$) [visible (Q_y)]	Forbidden
	$^1B_{2u}^*(^1E_u^*)$	Strongly allowed ($\theta \cong 90°$) [Soret (B_y)]	Forbidden
	$^1B_{3u}^*(^1E_u^*)$	Weak ($\theta \cong 0°$) [visible (Q_x)]	Forbidden
	$^1B_{3u}^*(^1E_u^*)$	Strongly allowed ($\theta \cong 0°$) [Soret (B_x)]	Forbidden
	$^1B_{1g}^*(^1B_{2g}^*)$	Forbidden	Allowed ($\Omega = 1.5$)
	$^1A_g^*(^1A_{1g}^*,^1B_{1g}^*)$	Forbidden	Strongly allowed ($\Omega \sim 1.0$)
C_s ("D_{4h}")	$^1A''^*("^1E_u^*")$	Weak (θ varies) [visible (Q_y,Q_x)]	Weak–strong ($\Omega \cong 1.25$)
	$^1A''^*("^1E_u^*")$	Strongly allowed (θ varies) [Soret (B_y,B_x)]	Weak–strong ($\Omega \cong 1.25$)
	$^1A'^*("^1B_{1g}^*")$	Weak–medium[d] (θ varies)	Weak–strong ($\Omega \cong 1.5$)
	$^1A'^*("^1B_{2g}^*")$	Weak–medium[d] (θ varies)	Weak–strong ($\Omega \cong 1.0$)
	$^1A'^*("^1A_{1g}^*")$	Weak[d] (θ varies)	Medium–strong ($\Omega \cong 1.5$)
C_s ("D_{2h}")	$^1A''^*("^1B_{2u}^*")$	Very weak (θ varies) [visible (Q_y)]	Very weak ($\Omega \cong 1.25$)
	$^1A''^*("^1B_{2u}^*")$	Medium–strong ($\theta \cong 15°$) [Soret (B_y)]	Weak ($\Omega \cong 1.25$)
	$^1A''^*("^1B_{3u}^*")$	Weak ($\theta \cong 90°$) [visible (Q_x)]	Very weak ($\Omega \cong 1.0$)
	$^1A''^*("^1B_{3u}^*")$	Medium–strong ($\theta \cong 20°$) [Soret (B_x)]	Weak–strong ($\Omega \cong 1.0$)
	$^1A'^*("^1B_{1g}^*")$	Weak–medium[e] (θ varies)	Weak–strong ($\Omega \cong 1.0$)
	$^1A'^*("^1A_g^*")$	Weak–medium[e] (θ varies)	Medium–strong ($\Omega \cong 1.0$)

[a] Symmetry of the excited state. Correlated D_{4h} symmetry species are given for the D_{2h} point group. The symmetry species for the C_s ("D_{4h}-like") and C_s ("D_{2h}-like") point groups are approximate and are assigned by correlation with the D_{4h} and D_{2h} point groups, respectively.

[b] Allowed or forbidden character of the one-photon transition. The polarization of the transition (θ) is defined relative to the axis defined by the nitrogens not bonded to hydrogen in the free bases and to the equivalent axis in the dianions (i.e., the x axis; see Fig. 1).

[c] Allowed or forbidden character of the two-photon transition. The two-photon polarization ratio (Ω) is defined in Table III.

[d] The intensity of the one-photon transition into " $^1B_{1g}^*$ ", " $^1B_{2g}^*$ ", and " $^1A_g^*$ " states is a function of the proximity and oscillator strength of " $^1E_u^*$ " states from which intensity is borrowed.

[e] The intensity of the one-photon transition into " $^1B_{1g}^*$ " and " $^1A_g^*$ " states is a function of the proximity and oscillator strength of " $^1B_{2u}^*$ " and " $^1B_{3u}^*$ " states from which intensity is borrowed.

TABLE III. Calculated one-photon oscillator strengths and two-photon absorptivities for the lowest-lying $\pi^* \leftarrow \pi$ transitions in free base porphin (FBP).[a,b]

$\Delta E(eV)$[c]	Symmetry[d]	f[e]	$\|\theta\|$[f]	$\langle A \rangle$[g]	$\langle B \rangle$[g]	$\langle C \rangle$[g]	$\langle D \rangle$[g]	Ω[h]
1.847	$^1B_{2u}^*$	$1.2E-03$	90	0	0	0	0	...
2.534	$^1B_{3u}^*$	0.062	0	0	0	0	0	1.259
3.134	$^1B_{1g}^*$	0	90	1.579	1.184	2.368	0.395	1.500
3.229	$^1B_{2u}^*$	0.321	90	0	0	0	0	...
3.259	$^1A_g^*$	0	19	13.763	10.073	20.146	3.690	1.464
3.460	$^1A_g^*$	0	2	1.054	0.766	1.532	0.288	1.453
3.490	$^1B_{3u}^*$	0.729	0	0	0	0	0	...
3.493	$^1B_{1g}^*$	0	0	0.610	0.458	0.916	0.153	1.500
3.816[i]	$^1A_g^*$	0	**88**	**585.715**	**71.943**	**143.886**	**513.771**	**0.246**
3.827	$^1B_{2u}^*$	1.304	90	0	0	0	0	...
3.838	$^1B_{1g}^*$	0	88	23.269	17.452	34.903	5.817	1.500
3.906	$^1B_{1g}^*$	0	68	(50.326)	(37.744)	(75.488)	(12.581)	1.500
3.984	$^1B_{3u}^*$	0.884	0	0	0	0	0	...

[a] Based on CNDO-π-SCF-MO-PSDCI calculations including full single and partial double excitation CI (see the text). The two-photon absorptivities are calculated using the 30 lowest energy intermediate states. The energies of the λ and μ photons are assumed to be equal and are calculated using the formula $E_\lambda = E_\mu = \Delta E / 2$.

[b] The crystal geometry (artificially constrained to planarity) of FBP is used. (See Refs. 6 and 32.)

[c] Transition energy relative to correlated ground state. State 1 is ground state.

[d] Symmetry of the electronic state. FBP belongs to the D_{2h} point group.

[e] Oscillator strength of the one-photon transition.

[f] Polarization of the one-photon transition relative to the x axis (as specified in Fig. 1).

[g] Two-photon absorptivities in cm^4 s molecule^{-1} photon^{-1} ($\times 10^{-50}$) for the polarization relationships defined in Table I. Absorptivities given in parentheses are significantly enhanced through resonance.

[h] The two-photon polarization ratio defined as $\langle C \rangle / \langle A \rangle$.

[i] Boldface type designates strongly two-photon allowed ($\langle A \rangle = 586$) Soret region $^1A_g^*$ state.

and FBP^{2-}, respectively), whereas the B states are found to contain significant contributions from configurations outside the four oribitals (43% and 83% four orbital localized for FBP and FBP^{2-}, respectively). Also in accord with results from earlier studies,[5,7,15,17] we predict that two degenerate E_u states contribute to the Soret band intensity for the dianion, whereas two or more states with high oscillator strength lie in the Soret region of FBP (see Fig. 3). Differentiation of B and higher-lying states (N states, characterized by low oscillator strengths) is thus more ambiguous for FBP than for FBP^{2-}.

Our calculations indicate that two-photon allowed

TABLE IV. Calculated one-photon oscillator strengths and two-photon absorptivities for the lowest-lying $\pi^* \leftarrow \pi$ transitions in free base porphin dianion (FBP^{2-}).[a,b]

$\Delta E(eV)$[c]	Symmetry[d]	f[e]	$\|\theta\|$[f]	$\langle A \rangle$[g]	$\langle B \rangle$[g]	$\langle C \rangle$[g]	$\langle D \rangle$[g]	Ω[h]
2.184	$^1E_u^*$	0.024	51	0	0	0	0	...
2.185	$^1E_u^*$	0.024	39	0	0	0	0	...
3.179	$^1B_{1g}^*$	0	13	(20.836)	(15.627)	(31.254)	(5.209)	1.500
3.519	$^1B_{2g}^*$	0	1	(1.685)	(1.264)	(2.527)	(0.421)	1.500
3.654	$^1E_u^*$	1.606	49	0	0	0	0	...
3.654	$^1E_u^*$	1.606	41	0	0	0	0	...
3.691	$^1B_{2g}^*$	0	0	29.342	22.006	44.012	7.336	1.500
3.943	^{1}"g^*"	0	12	(60.879)	(45.659)	(91.319)	(15.219)	1.500
3.986[i]	$^1A_{1g}^*$	0	**73**	**(125.870)**	**(15.734)**	**(31.468)**	**(110.137)**	**0.250**
3.995	$^1B_{1g}^*$	0	76	0	0	0	0	...
4.034	^{1}"g^*"	0	62	(0.080)	(0.011)	(0.022)	(0.069)	0.278
4.072	$^1B_{2g}^*$	0	60	160.089	120.065	240.130	40.024	1.500
4.120	$^1E_u^*$	0.046	65	0	0	0	0	...
4.120	$^1E_u^*$	0.047	26	0	0	0	0	...

[a] See footnote a of Table III.

[b] See footnote b of Table III.

[c] See footnote c of Table III.

[d] Symmetry of the electronic state. FBP^{2-} belongs to the D_{4h} point group. States which are mixtures of A_{1g}, B_{1g}, A_{2g}, and B_{2g} are labeled "g".

[e] See footnote e of Table III.

[f] See footnote f of Table III.

[g] See footnote g of Table III.

[h] See footnote h of Table III.

[i] Boldface type indicates state corresponding to the most strongly two-photon allowed state in FBP ($\langle A \rangle = 586$).

strongly allowed when accessed using linearly polarized photons ($\langle A \rangle = 585 \times 10^{-50}$ cm^4 s molecule^{-1} photon^{-1}). $^1B^*_{1g}(x,y)$ states in FBP are most strongly allowed under circularly ($\langle C \rangle$) polarized excitation. $^1A^*_{1g}(x^2 + y^2)$ states in FBP^{2-} are most strongly allowed under excitation from linearly polarized ($\langle A \rangle$) photons. Both $^1B^*_{1g}(x^2 - y^2)$ and $^1B^*_{2g}(xy)$ states possess their largest two-photon absorptivities upon excitation by circularly polarized ($\langle C \rangle$) photons.

Additional characteristics of $^1B^*_{1g}$ states (D_{2h}) and $^1B^*_{1g}$, $^1B^*_{2g}$, and $^1A^*_{1g}$ states (D_{4h}) arise from manifestations of specific symmetry relationships within the two-photon tensor elements. For $^1B^*_{1g}(D_{2h})$ and $^1B^*_{1g}$ and $^1B^*_{2g}(D_{4h})$ states the tensor element $S_{\alpha\alpha}S^*_{\beta\beta}$ is zero by symmetry. The two-photon polarization ratio $\langle C \rangle / \langle A \rangle$ then has an exact value of 3/2 (in the absence of vibronic coupling). In $^1A^*_{1g}$ states (D_{4h}) the following relationship holds due to symmetry considerations:

$$S_{\alpha\alpha}S^*_{\beta\beta} = S_{\alpha\beta}S^*_{\alpha\beta} + S_{\alpha\beta}S^*_{\beta\alpha}. \qquad (13)$$

The two-photon polarization ratio then has an exact value of 1/4 (in the absence of vibronic coupling). These polarization relationships are summarized in the following equations:

$$\Omega = \frac{3(S_{\alpha\beta}S^*_{\alpha\beta} + S_{\alpha\beta}S^*_{\beta\alpha}) - 2S_{\alpha\alpha}S^*_{\beta\beta}}{2(S_{\alpha\beta}S^*_{\alpha\beta} + S_{\alpha\beta}S^*_{\beta\alpha}) + 2S_{\alpha\alpha}S^*_{\beta\beta}}, \qquad (14a)$$

$$= \tfrac{3}{2} \qquad (S_{\alpha\alpha}S^*_{\beta\beta} = 0), \qquad (14b)$$

$$= \tfrac{1}{4} \qquad (S_{\alpha\beta}S^*_{\alpha\beta} + S_{\alpha\beta}S^*_{\beta\alpha} = S_{\alpha\alpha}S^*_{\beta\beta}). \qquad (14c)$$

The respective values of 3/2 and 1/4 are invariant to the relative photon energies since the tensor products $S_{\alpha\beta}S^*_{\alpha\beta}$ and $S_{\alpha\beta}S^*_{\beta\alpha}$ [Eqs. (7) and (8), respectively] are equally weighted.

B. Field effects on one- and two-photon properties

The effect of an external electric field on the one- and two-photon properties of porphyrins is of interest for three reasons. First, pulsed lasers used in two-photon spectroscopy may achieve high electric field values in their focused beam waists, inducing changes in one- and two-photon properties in the process of obtaining two-photon spectra. Theoretical field effect calculations provide a framework for predicting the expected magnitude and direction of the changes in molecular properties induced via laser interrogation. Second, the effect of polar substituents on one- and two-photon spectra may be evaluated approximately as a field induced perturbation of the molecular π-electron density. For example, a carbonyl group generates a state field of approximately 2×10^7 V/cm. Analysis of field effects may therefore prove useful in understanding the optical properties of porphyrins with polar substituents (see below). Third, porphyrins and their analogs incorporated into proteins show markedly different one-photon spectra than the same molecules in apolar hydrocarbon solvents. These spectral shifts may be due, in part, to field effects induced by nearby polar groups or salt bridges. Figures 4 and 5 illustrate that significant one- and two-photon spectral changes are predicted for porphyrins in the presence of static electric fields with intensities $> 10^7$

FIG. 2. Calculated (CNDO-π-SCF-MO-CI) one-photon oscillator strengths and two-photon absorptivities for free base porphin under complete single (SCI) or complete single, partial double (PSDCI) configuration interaction. The gerade or ungerade singlet electronic states are represented by darkened or undarkened rectangles, respectively, where the vertical position of the rectangle indicates the transition energy of the state, and the vertical width is linearly proportional to the one-photon oscillator strength (left two columns) and logarithmically proportional to the two-photon absorptivity (right two columns). Each column is individually scaled with respect to its largest one-photon oscillator strength or two-photon absorptivity. Of particular significance is the strongly two-photon allowed $^1A^*_g$ state lying at approximately 3.8 eV. The reduction of the visible-Soret splitting upon inclusion of doubly excited configurations is also notable.

states ($1\ ^1B^*_{1g}$ in FBP; $1\ ^1B^*_{1g}$ and $1\ ^1B^*_{2g}$ in FBP^{2-}) lie between the Q and B bands, and that many two-photon states lie in the Soret region and higher in both molecules. Some of these states are predicted to have large two-photon absorptivities, making experimental observation feasible. Photons of both linear ($\langle A \rangle$ and $\langle B \rangle$) and circular ($\langle B \rangle$, $\langle C \rangle$, and $\langle D \rangle$) polarization give comparable two-photon absorptivities for the $^1A^*_g$ (x^2, y^2) states of FBP. The most strongly two-photon allowed $^1A^*_g$ state in FBP is most

TABLE V. A comparison of experimental and theoretical state energies, oscillator strengths, relative state energies, and relative oscillator strengths for free base porphin[a] for CNDO-π-SCF-MO calculations utilizing single configuration only (SCI) and both single and double configuration (PSDCI).

Parameter[b] (ΔE in cm^{-1})	SCI	PSDCI	Experimental[c]
ΔE_{Q_y}	13 610	14 897	16 233
ΔE_{Q_x}	16 571	20 438	19 230
ΔE_{B_y}	25 309	26 043	
			$\Delta E_B = 25\,316$
ΔE_{B_x}	28 124	28 148	
$(\Delta E_{B_y} - \Delta E_{Q_x})$	8 738	5 605	6 086
$(\Delta E_{Q_x} - \Delta E_{Q_y})$	2 815	5 541	2 997
f_{Q_y}	0.0010	0.0012	0.0012
f_{Q_x}	0.105	0.062	0.0097
f_{B_y}	0.998	0.321	
			$f_B = 1.02$
f_{B_x}	2.425	0.729	
$\dfrac{f_{Q_y} + f_{Q_x}}{f_{B_y} + f_{B_x}}$	0.031	0.060	0.011
$\dfrac{f_{Q_y}}{f_{Q_x}}$	0.009	0.019	0.124

[a] See footnote b of Table III.

[b] Theoretical energy values of all states are for the system origins. In the case of the visible bands, calculated transition intensities correspond to the (0,0) bands, as the (0,1) band intensities are vibronically induced, and our calculations do not account for discrete vibronic features (see the text).

[c] Experimental values are taken from reported spectra [U. Eisner and R. P. Linstead, J. Chem. Soc. (London) **1955**, 3749 and V. M. Albers and H. V. Knorr, J. Chem. Phys. **4**, 422 (1936)]. Visible band energies and oscillator strengths are for the experimental (0,0) bands. Oscillator strengths and oscillator strength ratios are approximate because of difficulties in assigning peak half-maximum heights due to differences in base line on opposite sides of the peaks.

V/cm. Such field intensities are experienced by porphyrins embedded in proteins, as typical polar group-to-chromophore distances of <5 Å can generate field intensities greater than 5×10^7 V/cm. Indeed, in a recent theoretical study Eccles and Honig accurately reproduced the *in vivo* red shift of chlorophyll by placing protein "point charges" in close proximity to the chlorophyll plane.[12] Field effect calculations of the type we are reporting here may provide further insight into these biological electrochromic effects.

The focused laser radiation used in two-photon investigations will typically produce transient electric fields in the range 10^4–10^5 V/cm and field intensities from 10^6 to $> 10^7$ V/cm are possible.[19] As we will demonstrate below, these latter intensities are sufficient to induce observable changes in the transition energies and two-photon properties of the excited electronic states. Spectroscopists should consider the possibility of field induced changes in the electronic properties of any solute being probed by focused irradiation from pulsed lasers.

The effects of an external electric field on the electronic properties of porphyrins may be understood primarily in terms of mixing of electronic states with their parity (g,u) opposites. In FBP, for example, $^1B^*_{2u}$ and $^1B^*_{3u}$ states are mixed with $^1B^*_{1g}$ and $^1A^*_g$ states, resulting in nonzero one-photon oscillator strengths and two-photon absorptivities for all four states. At sufficiently high field strengths (1×10^7 V/cm and greater) state reordering is observed due to the

tendency of the applied field to stabilize "ionic" states and destabilize "covalent" states.

C. Porphyrins with conjugating substituent groups

Porphyrins with conjugating substituents formally belong to the C_s point group, but the electronic states retain a significant amount of "D_{2h}-like" (FBP) or "D_{4h}-like" (FBP^{2-}) character. The following discussion assigns states using D_{2h} or D_{4h} symmetry labels regardless of actual symmetry. All of the calculations include full single and extensive double CI unless noted otherwise.

Theoretically calculated one-photon spectra for 2,4-diformyl (DFFBP, DFFBP^{2-}) and 2,4-divinyl (DVFBP, DVFBP^{2-}) free bases and dianions are similar to those for FBP and FBP^{2-} in that they remain "porphyrin-like" (weak visible, strong ultraviolet bands—see Figs. 6–9 and Tables VI–IX). Furthermore, all four substituted species are predicted to have a large number of states with significant two-photon absorptivities. The one- and two-photon selection rules, and the two-photon polarization relationships expressed in Eqs. (14a)–(14c), relax upon symmetry lowering induced by the substituents. Q and B bands, degenerate in FBP^{2-}, are split in the substituted dianions due to a loss of degeneracy in $^1E^*_u$ states induced by the substituents. One-photon allowed states in all four substituted species are predicted to be significantly red shifted with respect to their
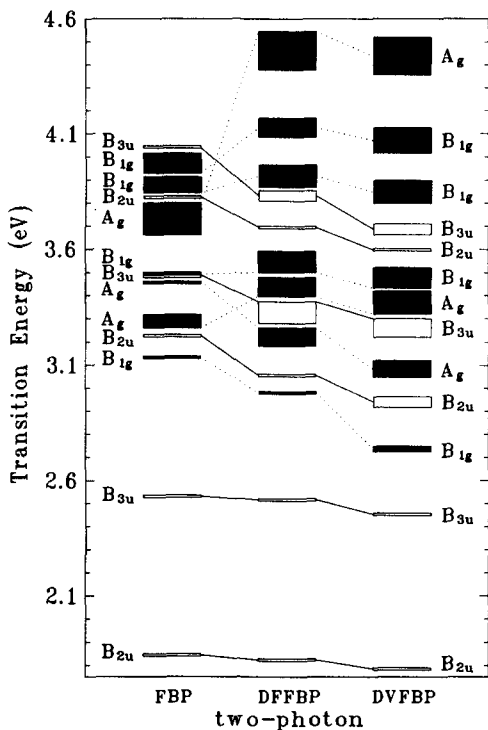
FIG. 3. Comparison of calculated (CNDO-π-SCF-MO-PSDCI) one-photon oscillator strengths and two-photon absorptivities of free base porphin dianion (FBP^{2-}) and free base porphin (FBP). One- and two-photon properties are represented as in Fig. 2. The loss of symmetry upon going from D_{4h} (FBP^{2-}) to D_{2h} (FBP) point groups removes degeneracy from states of E_u symmetry, causing the observed splitting. *Both* FBP^{2-} and FBP possess low-lying (Soret region) states with large two-photon absorptivities.

FIG. 5. Calculated (CNDO-π-SCF-MO-PSDCI) two-photon absorptivities for singlet excited states of free base porphin as a function of external electric field polarized along the axis defined by the nitrogens not bonded to hydrogen (the x axis). Two-photon properties are represented as in Fig. 2. State symmetry assignments are exact for $E_x = 0$ and approximate for $E_x \neq 0$.

FIG. 4. Calculated (CNDO-π-SCF-MO-PSDCI) one-photon oscillator strengths for singlet excited states of free base porphin as a function of external electric field polarized along the axis defined by the nitrogens not bonded to hydrogen (the x axis). One-photon properties are represented as in Fig. 2. State symmetry assignments are exact for $E_x = 0$ and approximate for $E_x \neq 0$.

FIG. 6. Comparison of calculated (CNDO-π-SCF-MO-PSDCI) one-photon oscillator strengths for singlet excited states of free base porphin (FBP), 2,4-diformyl free base porphin (DFFBP), and 2,4-divinyl free base porphin (DVFBP). One-photon properties are represented as in Fig. 2. State symmetry assignments are exact for FBP and approximate for DFFBP and DVFBP.

FIG. 7. Comparison of calculated (CNDO-π-SCF-MO-PSDCI) two-photon absorptivities for singlet excited states of free base porphin (FBP), 2,4-diformyl free base porphin (DFFBP), and 2,4-divinyl free base porphin (DVFBP). Two-photon properties are represented as in Fig. 2. Both substituted species posses many states with large two-photon absorptivities. State symmetry assignments are exact for FBP and approximate for DFFBP and DVFBP.
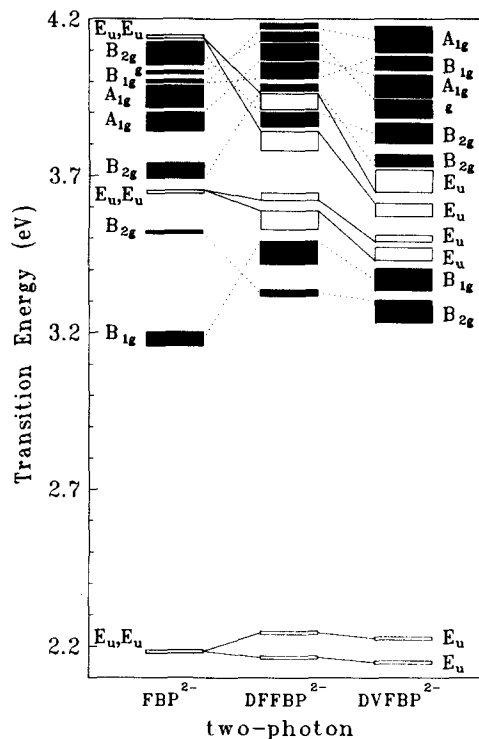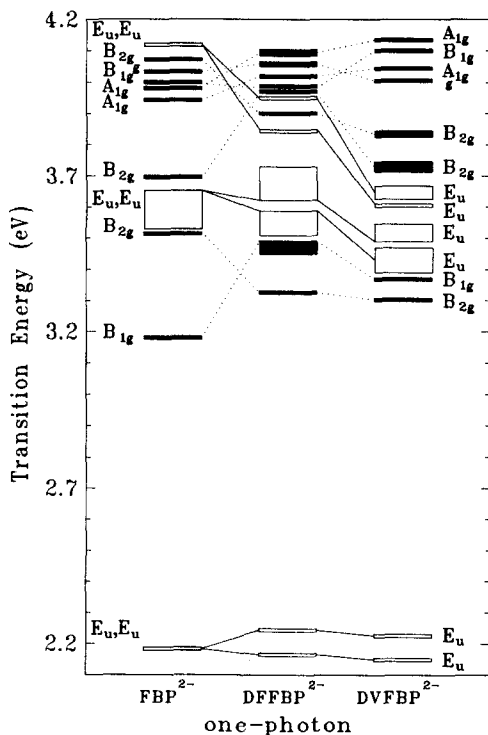

FIG. 9. Comparison of calculated (CNDO-π-SCF-MO-PSDCI) two-photon absorptivities for singlet excited states of freee base porphin dianion (FBP^{2-}), 2,4-diformyl free base porphin dianion ($DFFBP^{2-}$), and 2,4-divinyl free base porphin dianion ($DVFBP^{2-}$). Two-photon properties are represented as in Fig. 2. Both $DFFBP^{2-}$ and $DVFBP^{2-}$ possess many states with large two-photon absorptivities. State symmetry assignments are exact for FBP^{2-} and approximate for $DFFBP^{2-}$ and $DVFBP^{2-}$.

FIG. 8. Comparison of calculated (CNDO-π-SCF-MO-PSDCI) one-photon oscillator strengths for singlet excited states of free base porphin dianion (FBP^{2-}), 2,4-diformyl free base porphin dianion ($DFFBP^{2-}$), and 2,4-divinyl free base porphin dianion ($DVFBP^{2-}$). One-photon properties are represented as in Fig. 2. State symmetry assignments are exact for FBP^{2-} and approximate for $DFFBP^{2-}$ and $DVFBP^{2-}$.

corresponding states in FBP and FBP^{2-}. These results accord well with experimental data and are discussed in more detail below.

The configurational makeup of the Q and B state wave functions is predominantly four orbital in nature, though due to symmetry breakdown there is more contribution from configurations involving non-four-orbital excitations than there is in FBP and FBP^{2-}. The four orbitals are highly localized on the porphyrin macrocycle; and average of less than 3% of electron density in the four orbitals is localized on the substituents in all four substituted species. Hence, formyl and vinyl groups are predicted to induce *small* perturbations on porphyrin wave functions, even when assumed coplanar with the ring.

Our calculations predict that conjugative rather than polarity effects are primarily responsible for state mixing in the porphyrins. Selection rules are equally relaxed in the divinyl species ($\mu_0 = 0.29$ D for DVFBP; $\mu_0 = 0.19$ D for $DVFBP^{2-}$) and the diformyl species ($\mu_0 = 1.82$ D for DFFBP; $\mu_0 = 1.79$ D for $DFFBP^{2-}$), indicating that selection rule breakdown is induced mainly by conjugation of substituents into the ring, with substituent polarity playing a significantly lesser role. These results compare favorably with the UV-visible absorption spectra of 2,4-diformyldeuteroporphyrin IX dimethyl ester[38–40] (DFFBP-like) and protoporphyrin IX dimethyl ester[41] (DVFBP-like), in which the ϵ_Q/ϵ_B ratio is larger in the latter than the former, indicating a greater degree of symmetry breakdown or B–Q

TABLE VI. Calculated one-photon oscillator strengths and two-photon absorptivities for the lowest-lying $\pi^*\leftarrow\pi$ transitions in 2,4-diformyl free base porphin (DFFBP).[a,b]

$\Delta E(eV)$[c]	Symmetry[d]	f[e]	$\lvert\theta\rvert$[f]	$\langle A\rangle$[g]	$\langle B\rangle$[g]	$\langle C\rangle_g$	$\langle D\rangle$[g]	Ω[h]
1.852	" $^1B^*_{2u}$ "	0.8E-03	46	0.315	0.203	0.407	0.111	0.292
2.537	" $^1B^*_{3u}$ "	0.079	12	0.558	0.230	0.460	0.328	0.824
2.965	" $^1B^*_{1g}$ "	2.8E-03	19	0.456	0.339	0.678	0.117	1.486
3.097	" $^1B^*_{2u}$ "	0.208	82	2.002	1.466	2.933	0.536	1.465
3.313	" $^1A^*_{g}$ "	0.039	14	27.472	7.978	15.956	19.494	0.581
3.399	" $^1B^*_{3u}$ "	0.124	16	124.396	50.476	100.951	73.921	0.812
3.414	" $^1A^*_{g}$ "	0.322	6	28.600	8.044	16.089	20.556	0.563
3.495	" $^1B^*_{1g}$ "	0.064	37	(57.584)	(22.654)	(45.308)	(34.929)	0.787
3.725	" $^1B^*_{2u}$ "	1.429	84	0	2.375	4.750	0	...
3.860	" $^1B^*_{3u}$ "	1.164	2	5.692	3.868	7.737	1.824	1.359
3.933	" $^1B^*_{1g}$ "	0.032	30	(78.553)	(57.745)	(115.489)	(20.808)	1.470
4.134	" $^1B^*_{1g}$ "	0.035	10	34.682	6.544	13.088	28.138	0.377
4.569[i]	" $^1A^*_{g}$ "	6.5E-03	**61**	**(2183)**	**(1537)**	**(3074)**	**(645.9)**	**1.408**

[a] See footnote a of Table III.
[b] Coordinates for the porphyrin ring in DFFBP are assumed identical to those of FBP (see footnote b of Table III). Vinyl and formyl substituents are assigned standard geometries, with $R_{C-C} = 1.46$ Å, $R_{C=C} = 1.35$ Å, $R_{C=O} = 1.22$ Å, and bond angles of 120°.
[c] See footnote c of Table III.
[d] Approximate symmetry of the excited state. DFFB is "D_{2h}-like," although it formally belongs to the C_s point group.
[e] See footnote e of Table III.
[f] See footnote f of Table III.
[g] See footnote g of Table III.
[h] See footnote h of Table III.
[i] See footnote i of Table IV.

mixing in the DVFBP-like system. This result was not anticipated; theoretical studies of linear polyenes[19] indicate that polar groups mix excited states much more than nonpolar groups. It is, however, in agreement with the arguments of Adar[42] and of Hanson *et al.*[43] that the influences of substituents on porphyrins are due to conjugation into the ring and not to inductive effects on the prophyrin π orbitals. A direct inductive effect on macrocycle orbitals would result in greater mixing of states by formyl than by vinyl substituents. It is possible that neither vinyl nor formyl groups are sufficiently polar to perturb electron density within the porphyrin macrocycle.[44] The latter hypothesis would explain why vinyl and formyl groups mix states to an approximately equal extent.

TABLE VII. Calculated one-photon oscillator strengths and two-photon absorptivities for the lowest-lying $\pi^*\leftarrow\pi$ transitions in 2,4-diformyl free base porphin dianion (DFFBP^{2-}).[a,b]

$\Delta E(eV)$[c]	Symmetry[d]	f[e]	$\lvert\theta\rvert$[f]	$\langle A\rangle$[g]	$\langle B\rangle$[g]	$\langle C\rangle$[g]	$\langle D\rangle$[g]	Ω[h]
2.169	" $^1E^*_{u}$ "	0.028	51	0.394	0.291	0.582	0.104	1.474
2.249	" $^1E^*_{u}$ "	0.022	38	0.219	0.131	0.262	0.088	1.195
3.339	" $^1B^*_{2g}$ "	0.015	39	(5.393)	(0.685)	(1.371)	(4.707)	0.254
3.513	" $^1B^*_{1g}$ "	0.486	51	(210.399)	(157.733)	(315.466)	(52.666)	1.499
3.604	" $^1E^*_{u}$ "	1.126	58	(76.663)	(57.379)	(114.758)	(19.284)	1.497
3.644	" $^1E^*_{u}$ "	1.486	33	2.058	1.492	2.983	0.567	1.449
3.861	" $^1E^*_{u}$ "	0.018	28	(64.203)	(45.975)	(91.949)	(18.228)	1.432
3.902	" $^1B^*_{2g}$ "	0.047	69	14.979	7.674	15.348	7.305	1.025
3.969	" $^1E^*_{u}$ "	0.039	74	(31.419)	(20.388)	(40.776)	(11.031)	1.298
3.976	" $^1B^*_{2g}$ "	9.5E-03	43	(6.972)	(4.076)	(8.153)	(2.895)	1.169
3.994	" $^1B^*_{1g}$ "	0.061	21	(19.692)	(10.481)	(20.961)	(9.211)	1.064
4.019	" $^1g^*$ "	0.019	14	(30.568)	(21.552)	(43.103)	(9.016)	1.410
4.062	" $^1g^*$ "	0.179	34	(4.181)	(0.990)	(1.981)	(3.191)	0.474
4.100[i]	" $^1A^*_{1g}$ "	**0.248**	**60**	**(69.825)**	**(47.603)**	**(95.206)**	**(22.222)**	**1.364**

[a] See footnote a of Table III.
[b] Coordinates for the porphyrin ring in DFFBP^{2-} are assumed identical to those of FBP (see footnote b of Table III). Vinyl and formyl substituents are assigned standard geometries, with $R_{C-C} = 1.46$ Å, $R_{C=C} = 1.35$ Å, $R_{C=O} = 1.22$ Å, and bond angles of 120°.
[c] See footnote c of Table III.
[d] Approximate symmetry of the excited state. DFFBP^{2-} is "D_{4h}-like," although it formally belongs to the C_s point group.
[e] See footnote e of Table III.
[f] See footnote f of Table III.
[g] See footnote g of Table III.
[h] See footnote h of Table III.
[i] See footnote i of Table IV.

TABLE VIII. Calculated one-photon oscillator strengths and two-photon absorptivities for the lowest-lying $\pi^* \leftarrow \pi$ transitions in 2,4-divinyl free base porphin (DVFBP).[a,b]

ΔE (eV)[c]	Symmetry[d]	f[e]	$\lvert\theta\rvert$[f]	$\langle A\rangle$[g]	$\langle B\rangle$[g]	$\langle C\rangle$[g]	$\langle D\rangle$[g]	Ω[h]
1.787	" $^1B_{2u}^*$ "	0.9E-03	67	1.053	0.545	1.091	0.508	1.036
2.456	" $^1B_{3u}^*$ "	0.103	20	0.208	0.084	0.167	0.124	0.805
2.747	" $^1B_{1g}^*$ "	0.016	42	(5.953)	(2.900)	(5.801)	(3.053)	0.974
2.943	" $^1B_{2u}^*$ "	0.180	85	5.668	3.035	6.069	2.633	1.071
3.088	" $^1A_g^*$ "	0.049	16	11.301	5.980	11.960	5.321	1.058
3.303	" $^1B_{3u}^*$ "	0.218	19	(57.479)	(36.286)	(72.572)	(21.194)	1.262
3.325	" $^1A_g^*$ "	0.133	11	128.262	51.490	102.981	76.772	0.803
3.438	" $^1B_{1g}^*$ "	0.006	53	(52.865)	(24.804)	(49.608)	(28.061)	0.938
3.605	" $^1B_{2u}^*$ "	1.298	89	0	0	0	0	...
3.695	" $^1B_{3u}^*$ "	1.087	6	17.281	9.675	19.349	7.607	1.119
3.854	" $^1B_{1g}^*$ "	0.019	50	94.673	62.722	125.443	31.952	1.325
4.076	" $^1B_{1g}^*$ "	0.117	2	133.618	20.950	41.900	112.668	0.314
4.448[i]	" $^1A_g^*$"	**0.047**	**41**	**(1950)**	**(1470)**	**(2939)**	**(480.9)**	**1.507**

[a] See footnote a of Table III.

[b] Coordinates for the porphyrin ring in DVFBP are assumed identical to those of FBP (see footnote b of Table III). Vinyl and formyl substituents are assigned standard geometries, with $R_{C=C} = 1.46$ Å, $R_{C-C} = 1.35$ Å, $R_{C=O} = 1.22$ Å, and bond angles of 120°.

[c] See footnote c of Table III.

[d] Approximate symmetry of the electronic state. DVFBP is "D_{2h}-like," although it formally belongs to the C_s point group.

[e] See footnote e of Table III.

[f] See footnote f of Table III.

[g] See footnote g of Table III.

[h] See footnote h of Table III.

[i] See footnote i of Table IV.

The resonance Raman studies of Willems and Bocian[45] indicate that conjugating substituents are capable of influencing the axis systems of the transition moment vectors for the Q_y and Q_x bands in metalloporphyrins. These studies suggest that disubstitution of conjugating substituents on adjacent pyrrole rings introduces more asymmetry into the electronic structure than does monosubstitution. In accord with these studies, our preliminary calculations on 2- and 4-monoformyl FBP^{2-} indicate that $\langle Q_x \lvert r \rvert S_0\rangle$ and $\langle Q_y \lvert r \rvert S_0\rangle$ lie approximately through adjacent pyrrole rings. In contrast, the axis system of DFFBP^{2-} is rotated with respect to the monoformyl axis systems so that $\langle Q_x \lvert r \rvert S_0\rangle$ and $\langle Q_y \lvert r \rvert S_0\rangle$ are directed approximately through adjacent *methine* bridges. Such a rotation of the axis system would be expected to cause excited state vibrations to be nonorthogonal to their corresponding ground state vibrations (i.e., it

TABLE IX. Calculated one-photon oscillator strengths and two-photon absorptivities for the lowest-lying $\pi^* \leftarrow \pi$ transitions in divinyl free base porphin dianion (DVFBP^{2-}).[a,b]

ΔE (eV)[c]	Symmetry[d]	f[e]	$\lvert\theta\rvert$[f]	$\langle A\rangle$[g]	$\langle B\rangle$[g]	$\langle C\rangle$[g]	$\langle D\rangle$[g]	Ω[h]
2.151	" $^1E_u^*$ "	0.042	74	1.004	0.714	1.429	0.289	1.423
2.226	" $^1E_u^*$ "	0.036	14	0.332	0.196	0.392	0.135	1.184
3.311	" $^1B_{2g}^*$ "	0.051	70	(102.251)	(74.714)	(149.428)	(27.537)	1.461
3.379	" $^1B_{1g}^*$ "	0.114	30	(145.456)	(108.277)	(216.553)	(37.179)	1.489
3.440	" $^1E_u^*$ "	1.048	66	14.823	11.112	22.225	3.711	1.499
3.500	" $^1E_u^*$ "	0.776	27	36.772	15.559	31.118	21.213	0.846
3.626	" $^1E_u^*$ "	0.143	34	(8.955)	(5.229)	(10.599)	(3.656)	1.184
3.658	" $^1E_u^*$ "	0.533	33	(111.232)	(53.346)	(106.693)	(57.886)	0.959
3.738	" $^1B_{2g}^*$ "	0.405	62	7.661	1.598	3.195	6.063	0.417
3.844	" $^1B_{2g}^*$ "	0.237	29	(42.564)	(26.956)	(53.911)	(15.608)	1.266
4.007	" $^1g^*$"	0.032	78	44.541	33.343	66.686	11.198	1.497
4.044	" $^1g^*$"	0.026	69	(127.120)	(87.189)	(174.378)	(39.931)	1.372
4.101	" $^1B_{2g}^*$ "	0.018	68	(17.370)	(12.146)	(24.292)	(5.224)	1.398
4.135[i]	" $^1A_{1g}^*$ "	**1.0E-03**	**27**	**(295.503)**	**(226.901)**	**(453.802)**	**(68.602)**	**1.536**

[a] See footnote a of Table III.

[b] Coordinates for the porphyrin ring in DVFBP^{2-} are assumed identical to those of FBP (see footnote b of Table III). Vinyl and formyl substituents are assigned standard geometries, with $R_{C-C} = 1.46$ Å, $R_{C=C} = 1.35$ Å, $R_{C=O} = 1.22$ Å, and bond angles of 120°.

[c] See footnote c of Table III.

[d] Approximate symmetry of the electronic state. DVFBP^{2-} is "D_{4h}-like," although it formally belongs to the C_s point group.

[e] See footnote e of Table III.

[f] See footnote f of Table III.

[g] See footnote g of Table III.

[h] See footnote h of Table III.

[i] See footnote i of Table IV.

would be expected to induce Duschinsky rotation of the excited states) introducing a greater degree of asymmetry into the electronic structure of the disubstituted relative to the monosubstituted species.

Willems and Bocian[45] observed Q_x–Q_y energy splittings of 300–400 cm^{-1} for both 2- or 4-monoformyl and 2,4-diformyl nickel porphyrins. We obtain theoretical values within this range for the monosubstituted systems ($\Delta E_{Q_xQ_y} = 366$ and 367 cm^{-1} for monoformyl FBP^{2-} and monovinyl FBP^{2-}, respectively) and obtain larger values for the disubstituted systems ($\Delta E_{Q_xQ_y} = 645$ cm^{-1} for DFFBP^{2-} and 605 cm^{-1} for DVFBP^{2-}). The larger splittings for the disubstituted systems reflect the greater nonequivalence of transition moment axes in the diformyl and divinyl systems due to the presence of more than one substituent. Interestingly, calculations on the dianions utilizing single CI only yield Q_x–Q_y splittings of approximately 10 cm,$^{-1}$ indicating that most of the difference in energy between Q_x and Q_y bands is attributable to double CI contributions to the wave functions.

Calculated red shifts for the visible and Soret states of DFFBP and DVFBP with respect to FBP are of the same order of magnitude ($\Delta\lambda \simeq 30$ nm) as those observed experimentally (for 2,4-diformyldeuteroporphyrin IX dimethyl ester[38–40] and protoporphyrin IX dimethyl ester[41] with respect FBP,[46] respectively). Our calculated red shifts are larger for DVFBP than for DFFBP, in direct contrast to the experimental data. Changing oxygen parametrization (ionization potentials, $\langle ii|ii \rangle$ values, and β^0 bonding parameters) yield no significant improvement in the red shifts for DFFBP reported here. However, calculated changes in dipole moment $\Delta\mu_{0i}$ from ground (0) to excited (*i*) states for both DFFBP and DVFBP are much larger than the corresponding dipole moment changes in FBP. Our calculations are for molecules in vacuum, and do not account for changes in transition energies induced by solvent environment. We speculate, therefore, that the experimental red shifts of 2,4-diformyldeuteroporphyrin IX dimethyl ester and protoporphyrin IX dimethyl ester are primarily due to solvent-induced lowering of energies of states with large $\Delta\mu_{0i}$ values, with a smaller amount of red shift originating from conjugation-induced enlargement of the effective ring radius or inductive effects altering porphyrin π-orbital energies. The same arguments apply to the porphyrin dianions (metalloporphyrins).

Solvent-induced red shifts accord well with recent NMR studies of vinyl-substituted porphyrins which suggest that vinyl groups lie approximately 50° out of the porphyrin plane[47] in solution, significantly reducing the amount of possible enlargement of the ring by in-plane conjugation. Solvent-induced red shifts also agree with recent experimental work by Renge *et al.*,[48] who report that protic solvents cause red shifting of the Q bands of chlorophyll *a*, and by Ward *et al.*,[49] who report that the amount of visible and Soret band red shift is strongly dependent upon substituent polarity and solvent for various formyl-, Schiff base-, and protonated Schiff base-substitued porphyrinoid compounds.

A comparison of Figs. 4 and 5 with Figs. 6 and 7 reveals that both the magnitude and direction of the effects of elec-

tric field on state energies and one-photon oscillator strengths may differ, sometimes greatly, from the effects caused by formyl substituents (see Sec. III B). The effects of electric field and of formyl substituents on two-photon absorptivity values are quite similar however, because two-photon allowedness is largely a function of change in dipole moment upon excitation,[33–35] and both external field and the presence of substituents contribute to large $\Delta\mu_{0i}$ values. Conjugative and solvent effects are both significant factors in determining the electronic properties of these systems. It is thus legitimate to describe the influence of formyl substituents as a field effect to a first approximation only.

D. Two-photon spectroscopy of porphyrins

It is now well established that two-photon studies of polyenes and amino acids have provided important new insights into the electronic structure of these compounds not apparent from detailed studies of the allowed excited states.[28,36,50–57] Two-photon spectroscopy has been particularly useful for the analysis of low-lying forbidden states in compounds such as the retinyl polyenes, which display severe inhomogeneous broadening.[28,36,54–57] The recent application of two-photon thermal lensing to study the chromophore binding site of rhodopsin[54] indicates that the assignment of forbidden states can provide important insights into the electrostatic nature of binding sites.[36,54]

The calculations reported in this paper suggest that the low-lying forbidden states of porphyrins share many of the same characteristics that have been observed for the low-lying forbidden states in polyenes.[36,51] In particular, low-lying, strongly two-photon allowed states are present in porphyrins, and these states are highly sensitive to environment (see Fig. 5). This observation suggests that two-photon spectroscopy may prove useful in analyzing the binding sites of protein bound porphyrins and chlorins (see Ref. 36).

The two-photon absorptivities of the low-lying two-photon allowed states are relatively large. In general, a two-photon allowed excited state is considered to be experimentally observable via standard experimental techniques if it has an absorptivity on the order of 10^{-50} cm^4 s molecule^{-1} photon^{-1}.[50] Examination of Tables III–IX indicates that a majority of the two-photon allowed states meet this criterion, and more importantly, the "indicator" forbidden states have absorptivities that are 1–3 orders of magnitude larger. The latter states, which would be important to locate if one were to use two-photon spectroscopy to analyze environmental effects, should be very easy to detect experimentally, even in nonfluorescing systems. (The two-photon allowed states observed in the retinyl polyenes have absorptivities that are typically tenfold smaller.[28,36,54,56,57]) We anticipate, based on the results reported in this paper, that two-photon spectroscopy of porphyrins will play an increasingly important role in the analysis of the electronic properties of these molecules, both in solution and in protein environment.

IV. SUMMARY AND CONCLUSIONS

Our analysis of the above calculations on free base porphin, free base porphin dianion, and the 2,4-diformyl and

2,4-divinyl analogs of these compounds lead to the following conclusions:

(1) Free base porphin, free base porphin dianion, and their 2,4-diformyl and 2,4-divinyl analogs are all predicted to have low-lying (gerade) states with large two-photon absorptivities. Based on the similarities between porphyrin dianions and metalloporphyrins in other theoretical studies[5,6,14] we expect that the large two-photon absorptivities associated with the dianions are genuine and not due to a failure to include metal parametrization. It should therefore prove feasible experimentally to obtain two-photon excitation or thermal lens spectra of many naturally occurring and synthetic metalloporphyrins and free base porphyrins, both in solution and in protein binding sites.

(2) The two-photon absorptivities of porphyrins cannot be accurately described using the single intermediate state approximation, a formalistic approximation that proved viable for a majority of nonpolar polyenes.[19] At least 10 (and often >20) excited states must be included in the summation over intermediate states to reach convergence of the two-photon tensor calculation.

(3) The inclusion of extensive double configuration interaction significantly improves the calculated energy difference between the visible and Soret bands, and the Q band oscillator strengths, over calculations which utilize extensive single configuration interaction only.

(4) State mixing caused by substituents conjugating into the ring is the primary cause of selection rule relaxation in the porphyrins; direct inductive effects on macrocycle orbitals are of minor importance in this regard. Our results support earlier work by Hanson et al.,[43] who concluded that polar groups perturb states more than nonpolar groups, but by means of a conjugative, rather than inductive, effect. Substituent polarity alone is not a clear indicator of whether or not states will be strongly mixed. Polar substituents will strongly mix states only when substituent orbitals are lowered into the energy region of the macrocycle LUMOs (in the examples described by Hanson et al.[43] this latter effect is observed when polar Schiff base substituents are protonated).

(5) The orientation of the transition dipole vectors in disubstituted porphyrin dianions (metalloporphyrins) with conjugating substituents on adjacent pyrrole rings is significantly rotated with respect to that of monosubstituted porphyrin dianions (metalloporphyrins).

(6) Enlargement of the effective porphyrin ring radius and inductive effects on macrocycle π orbitals account for only part of the red shift in the one-photon spectra of porphyrins having conjugating substituents with respect to their unsubstituted counterparts. A substantial portion of the red shift may be due to solvent lowering of the ground-to-excited state energy difference because of large changes in dipole moment upon excitation in the substituted species.

[1] (a) M. Gouterman, *The Porphyrins*, edited by D. Dolphin (Academic, New York, 1978), Vol. III, pp. 1–165; (b) F. Adar, *ibid.* pp. 167–209; (c) C. Weiss, *ibid.* pp. 211–223.

[2] (a) G. H. Loew, *Iron Porphyrins*, edited by A. B. P. Lever and H. B. Gray (Addison–Wesley, Reading, MA, 1983), Part 1, pp. 1–87; (b) M. W. Makinen and A. K. Churg, *ibid.* pp. 141–235.

[3] M. Gouterman, J. Chem. Phys. 30, 1139 (1959).

[4] M. Gouterman, J. Mol. Spectrosc. 6, 138 (1961).

[5] C. Weiss, H. Kobayashi, and M. Gouterman, J. Mol. Spectrosc. 16, 415 (1965).

[6] M. Zerner and M. Gouterman, Theor. Chim. Acta 4, 44 (1966).

[7] A. J. McHugh, M. Gouterman, and C. Weiss, Jr., Theor. Chim. Acta 24, 346 (1972).

[8] D. C. Rawlings, E. R. Davidson, and M. Gouterman, Theor. Chim. Acta 61, 227 (1982).

[9] H. Sekino and H. Kobayashi, J. Chem. Phys. 75, 3477 (1981).

[10] C. Weiss, Jr., J. Mol. Spectrosc. 44, 37 (1972).

[11] W. D. Edwards and M. C. Zerner, Int. J. Quantum. Chem. 23, 1407 (1983).

[12] J. Eccles and B. Honig, Proc. Natl. Acad. Sci. U.S.A. 80, 4959 (1983).

[13] G. M. Maggiora, J. Am. Chem. Soc. 95, 6555 (1973).

[14] G. M. Maggiora and L. J. Weimann, Chem. Phys. Lett. 22, 297 (1973).

[15] J. D. Petke, G. M. Maggiora, L. L. Shipman, and R. E. Christoffersen, J. Mol. Spectrosc. 71, 64 (1978).

[16] J. D. Petke, G. M. Maggiora, L. L. Shipman, and R. E. Christoffersen, J. Mol. Spectrosc. 73, 311 (1978).

[17] R. E. Christoffersen, Int. J. Quantum Chem. 16, 573 (1979).

[18] J. D. Petke, G. M. Maggiora, L. L. Shipman, and R. E. Christoffersen, Photochem. Photobiol. 33, 663 (1981).

[19] R. R. Birge and B. M. Pierce, J. Chem. Phys. 70, 165 (1979).

[20] This technique differs from that used in earlier two-photon calculations (PPP-SCF-CISD) in that overlap integrals are approximated via a Mulliken formalism utilizing Slater exponents [see R. S. Mulliken, C. A. Rieke, D. Orloff, and H. Orloff, J. Chem. Phys. 17, 1248 (1949)]. In this method, C=C, C=N, and C=O overlap integrals have different values at a given bond distance. In the earlier method, overlap was assigned to all three bond types using a linear approximation to a standard C=C overlap integral function, giving C=C, C=N, and C=O bonds identical overlap values.

[21] K. Schulten, I. Ohmine, and M. Karplus, J. Chem. Phys. 64, 4422 (1976).

[22] P. Tavan and K. Schulten, J. Chem. Phys. 70, 5407 (1979).

[23] P. Tavan and K. Schulten, J. Chem. Phys. 70, 5414 (1979).

[24] K. Schulten, Ph.D. thesis, Harvard University, 1975.

[25] A. Schweig, Chem. Phys. Lett. 1, 163 (1967).

[26] H. Suzuki, *Electronic Absorption Spectra and Geometry of Organic Molecules* (Academic, New York, 1967), pp. 228–245.

[27] J. L. Hoard, M. J. Tamor, and T. A. Tamor, J. Am. Chem. Soc. 85, 2334 (1963).

[28] R. R. Birge, J. A. Bennett, L. M. Hubbard, H. L. Fang, B. M. Pierce, D. S. Kliger, and G. E. Leroi, J. Am. Chem. Soc. 104, 2519 (1982).

[29] W. L. Peticolas, Annu. Rev. Phys. Chem. 18, 233 (1967).

[30] W. M. McClain, Acc. Chem. Res. 7, 129 (1974).

[31] P. R. Monson and W. M. McClain, J. Chem. Phys. 53, 29 (1970).

[32] A. Gold, *Proceedings of the International School of Physics*, edited by R. J. Glauber (Academic, New York, 1969), pp. 397–420.

[33] W. M. McClain, J. Chem. Phys. 55, 2789 (1971).

[34] O. Sonnich Mortensen and E. Nørby Svendsen, J. Chem. Phys. 74, 3185 (1981).

[35] B. Dick and G. Hohlneicher, J. Chem. Phys. 76, 5755 (1982).

[36] R. R. Birge, Acc. Chem. Res. (in press).

[37] The calculated energy maxima of the visible bands corresponds to the (0,0) transitions (Franck–Condon allowed) only, and not to the (0,1) transitions (vibronically allowed), as our calculations do not account for vibronic effects. The visible bands may therefore be represented as single Gaussian profiles.

[38] P. S. Clezy and J. Barnett, Biochem. J. 78, 798 (1961), cited in *Porphyrins*

and Metalloporphyrins, edited by K. M. Smith (Elsevier, Amsterdam, 1975), p. 872.

[39]R. Lemberg and J. Parker, Aust. J. Expt. Biol. **30**, 163 (1952); p. 873.

[40]F. Sparatore and D. Mauzerall, J. Org. Chem. **25**, 1073 (1960); p. 873.

[41]J. E. Falk, *Porphyrins and Metalloporphyrins* (Elsevier, Amsterdam, 1964); p. 872.

[42]F. Adar, Arch. Biochem. Biophys. **170**, 644 (1975).

[43]L. K. Hanson, C. K. Chang, B. Ward, P. M. Callahan, G. T. Babcock, and J. D. Head, J. Am. Chem. Soc. **106**, 3950 (1984).

[44]Hanson *et al.* (Ref. 43) performed calculations on various disubstituted porphyrins with vinyl, Schiff base, carbonyl, and protonated Schiff base substituents. Their calculations indicate that substituent orbitals are too high in energy to mix with macrocycle LUMOs unless the substituent is protonated. In such cases, the localized charge preferentially stabilizes substituent orbitals, allowing them to mix with the LUMOs of the macrocycle, and thus "conjugate" into the ring. The LUMOs, which are approximately degenerate in the unprotonated species, become nondegenerate upon protonation, causing mixing between the B and Q states.

[45](a) D. L. Willems and D. F. Bocian, J. Am. Chem. Soc. **106**, 880 (1984); (b) J. Phys. Chem. **89**, 234 (1985).

[46]U. Eisner and R. P. Linstead, J. Chem. Soc. (London) **1955**, 3749.

[47]A. A. Bothner-By, C. Gayathi, P. C. M. van Zijl, C. MacLean, J-J. Lai, and K. M. Smith, Magn. Reson. Chem. **23**, 935 (1985).

[48]I. Renge, U. Moelder, and I. Koppel, Spectrochim. Acta Part A **41**, 967 (1985).

[49]B. Ward, C. K. Chang, and R. Young, J. Am. Chem. Soc. **106**, 3943 (1984).

[50]R. R. Birge, *Ultrasensitive Laser Spectroscopy*, edited by D. S. Kliger (Academic, New York, 1983), pp. 109–174.

[51]B. S. Hudson, B. E. Kohler, and K. Schulten, *Excited States*, edited by E. C. Lim (Academic, New York, 1982), Vol. 6, pp. 1–95.

[52]J. S. Horwitz, B. E. Kohler, and T. A. Spiglanin, J. Chem. Phys. **83**, 2186 (1985).

[53]B. E. Anderson, R. Jones, A. Rehms, P. Illich, and P. R. Callis, Chem. Phys. Lett. (in press).

[54]R. R. Birge, L. P. Murray, B. M. Pierce, H. Akita, V. Balogh-Nair, L. A. Findsen, and K. Nakanishi, Proc. Natl. Acad. Sci. U.S.A. **82**, 4117 (1985).

[55]D. S. Kliger, in *The Physics Teacher*, February, 1985, pp. 75–80.

[56]R. R. Birge, J. A. Bennett, B. M. Pierce, and T. M. Thomas, J. Am. Chem. Soc. **100**, 1533 (1978).

[57]L. P. Murray and R. R. Birge, Can. J. Chem. **63**, 1967 (1985).